8.2-dB Improvement of SNR in a Self-Mix Laser Diode Interferometer by using the Difference Signal at the Output Mirrors (Invited Paper)

Silvano Donati[1*] and Michele Norgia[2]

[1]*Department of Industrial and Information Engineering, University of Pavia, v. Ferrata 1, 27100 Pavia, Italy,*

[2]*Department of Electronics, Informatics and Bioengineering, Politecnico di Milano, p.za L. da Vinci 32, 20133 Milano, Italy.*

*Corresponding author: silvano.donati@unipv.it

Received Month X, XXXX | Accepted Month X, XXXX | Posted Online Month X, XXXX

Abstract At the mirrors of a Laser-Diode Self-Mixing Interferometer, the output beams carry anti-correlated (i.e., in phase opposition) interferometric signals, whereas the superposed noise fluctuations are (partially) correlated. Therefore, by using as an instrumental output of the interferometer the difference of the two, we double the amplitude of the self-mixing useful signal while the superposed noise is reduced. To validate the idea, we first calculate the noise reduction by means of a second-quantization model, finding that in a laser diode the SNR can be improved by 8.2-dB, typically. Then, we also carry out an experimental measurement of SNR and find very good agreement with the theoretical result.

Keywords: Interferometry, Self-Mixing, Noise, Laser diodes

1. Introduction

The Self-Mixing Interferometer (SMI) is a well-known minimum-part configuration of interferometry based on the modulations of the cavity field induced by the weak return from the target under measurement [1]. The modulation indexes are the signals cos 2kΔs and sin 2kΔs (with k=2 π/λ and s=distance to the target) for the AM (amplitude modulation) and FM (frequency modulation) respectively, that are necessary to trace back unambiguously the displacement Δs [2]. As the process is coherent, the SMI can work well even with very minute returns (e.g. down to 10^{-8} of emitted power) and this feature, coupled to the simplicity of the setup (no external optical parts required in principle) has led to the development of a number of applications of SMI, in the fields of mechanical metrology, biomedical signal sensing, physical quantity measurements and consumer products, see e.g. Ref. [1,3] for reviews.

About detection and processing of the modulated signal, usually the AM component is preferred because readily available on the laser beam power, and conveniently detected by the monitor photodiode usually provided by the manufacturer on the rear mirror of the laser package. Using the AM modulation, we can make digital or analogue processing of the SMI signal, respectively to count fringes of half-wavelength for displacement measurement and or to sense vibrations with an output analogue replica of the signal s(t) waveform, down to fraction of the wavelength and even much less with appropriate circuits [2,3].

One specific feature of the SMI is that the interferometric signal is carried by the beam, and is found not only on the rear output where the monitor photodiode PD2 is placed (see Fig.1), but also on the front output, where it can be picked up by a beamsplitter (BS) and photodiode PD1, as well as on the target itself (not shown in Fig.1) and on the returning beam by means of photodiode PD1'.

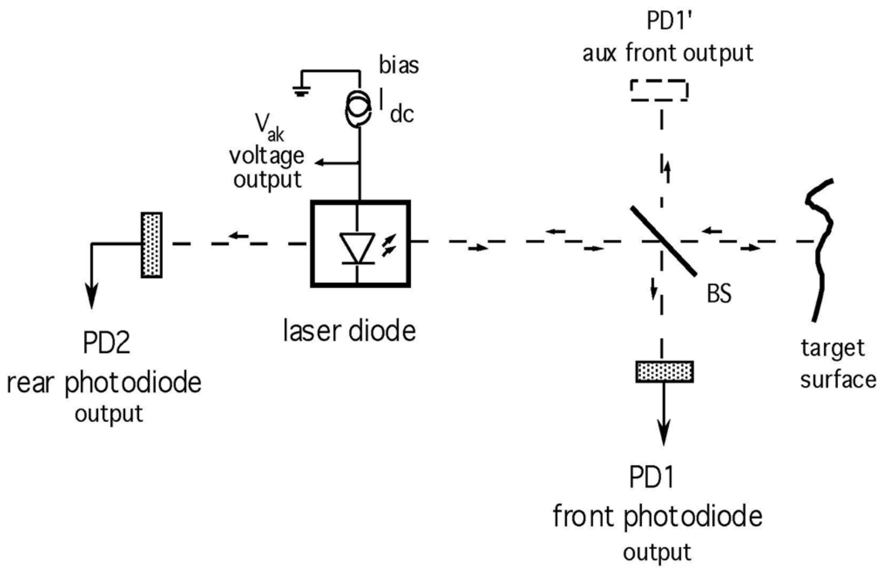

Fig. 1. Different pickups of the output signal from a self-mixing interferometer: from rear PD2 and from front mirror, PD1 and PD1'.

Placing the detecting photodiode on the target allows to exploit a unique property of the SMI, namely measuring the displacement or vibration of a target from the target location itself while it's moving – but this possibility will not be developed in this paper. Another special feature of SMI with semiconductor laser is the availability of the signal across the anode-cathode terminals of the laser diode (not shown in Fig.1) that in this case works also as a detector – a feature demonstrated for SMI operation at THz frequency [4]. More commonly, however, it's the rear photodiode PD2 signal to be used, because it is normally already available in the laser diode package and it doesn't obstruct the path of propagation to the remote target.

Also, the placement of the detector on the front beam output is interesting, because the signal here is in phase opposition to that detected at the rear mirror in semiconductor laser diodes driven well above threshold, as found by the analysis presented in Ref. [5].

Therefore, making the difference signal of the two outputs, the amplitude of the SMI signal improves of a factor of 2, as experimentally verified in Ref.[6].

Additionally, it is reasonable to expect that the two outputs, which are generated by the same optical field E_0 travelling back and forth in the laser cavity, are affected by the same noise carried by E_0 (that is to say, the two output noises are correlated) and thus the difference signal has less noise than the two SMI signals, or its SNR (signal-to-noise) ratio is furtherly improved.

If this conjecture proves correct, the performance of the SMI are improved in its ultimate sensitivity or detectable NED (noise-equivalent-displacement) [2].

In this paper we analyze the noise of the two outputs (front and rear) and of their difference with a semiclassical noise model [7] which accounts for second quantization and finds that indeed the two outputs have a partial correlation of noise and that the SNR can be improved up to about 10 dB by the differential signal. Then we test the theoretical results with a 650-nm laser diode SMI and are able to measure an 8.2 dB improvement of SNR, in good agreement with theory.

2. Theoretical Model and Analysis

To avoid unnecessary complications, we consider the simplified scheme of Fig.2 to evaluate signal and noise of the front and rear outputs of the laser diode, with the photodetectors placed directly on the outputs of the laser. The power reflectivity of mirrors M1 and M2 are R_1 and R_2, the power exiting from mirrors are P_1 and P_2, and they are converted into electrical current signals $I_1= \sigma P_1$ and $I_2= \sigma P_2$ by photodiodes PD1 and PD2. We suppose PD2 totally absorbing and PD1 partially reflecting, so as to act as the target and generate the feedback field re-entering the laser cavity after propagation to distance s and the accumulated optical phase shift ϕ=2ks.

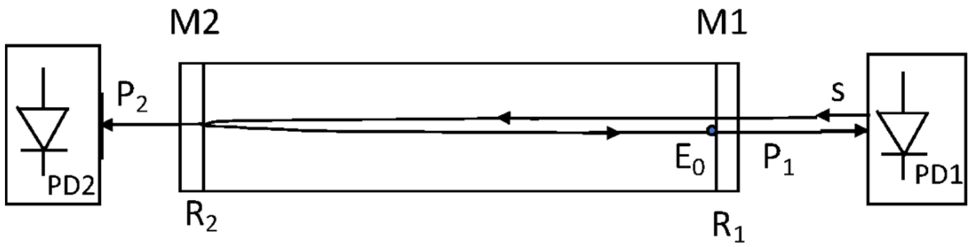

Fig.2. Simplified scheme of an SMI for the evaluation of front and rear outputs signal and noise.

The output power P is related to the electrical field amplitude E by the well-known Poynting's relation $P=aE^2/2Z_0$, where a is the cross-section area of the beam and Z_0 is the vacuum impedance. In the following however, we write simply $P_1=E_1^2$ and $P_2=E_2^2$ for the powers exiting at mirrors M1 and M2.

Now, we want to calculate the quiescent amplitude of the fields E_1 and E_2 as a function of the unperturbed internal field E_0, and their SMI amplitude variations ΔE_1 and ΔE_2 due to a feedback from the target at distance s returning into the cavity a fraction A of the field E_0 (taken just before M1, see Fig.2). The problem was solved in Ref. [5] with the following result for the output field amplitudes E_1 and E_2 when perturbed by a small return AE_0 from the target along a phase shift ϕ =2ks:

$$E_1= t_1 E_0 \{1 - (t_1^2/r_1) (A \cos \phi) [(2\gamma L + \ln R_1R_2)^{-1} - R_1/T_1]\} \tag{1}$$

$$E_2 = \sqrt{(r_1/r_2)}\, t_2 E_0 \{1- (t_1^2/r_1) (A \cos \phi) (2\gamma L + \ln R_1R_2)^{-1}\} \tag{2}$$

where:

A is the attenuation suffered by the field signal on the go-and-return path;

ϕ= 2ks is the optical phase accumulated in the path to the target and back, with $k=2\pi/\lambda$ the wavevector and s the target distance;

$r_{1,2} =\sqrt{R_{1,2}}$ and $t_{1,2} =\sqrt{R=T_{1,2}}$ are the field reflection and transmission of mirrors M1 and M2, respectively;

$2\gamma L$ is the round-trip gain along the laser cavity of length L,
and factor 1 in curl parentheses indicate the quiescent (or unperturbed) value of the field, to which the AM modulation term induced by the self-mixing is added.
From Eqs.1 and 2, we can calculate the modulation m_1 and m_2, defined as the ratio of SMI signal (the term added to unity) and the constant unperturbed field superposed to them, $E_{1,2}$ for A=0, and the result is

$$m_1= (t_1^2/r_1) (A \cos \phi) [(2\gamma L + \ln R_1R_2)^{-1} - R_1/T_1] \quad (3)$$

$$m_2 = (t_1^2/r_1) (A \cos \phi) (2\gamma L + \ln R_1R_2)^{-1}. \quad (4)$$

hence the ratio:

$$m_1/m_2 =1-(R_1/T_1)(2\gamma L+\ln R_1R_2) \quad (5)$$

Because of Eq.5, the outputs are in phase ($m_1/m_2 =1$) at threshold ($2\gamma L=-\ln R_1R_2$) then in normal operating conditions above threshold, $2\gamma L+\ln R_1R_2> T_1/R_1$, the outputs become in phase opposition (m_1/m_2 negative, typically $\approx$ -3). The difference in modulation indexes of rear and front output is explained by the extra contribution, in the front output, coming from the reflection, on the front mirror, of the field returning from the remote target.
In practical operation of a laser diode, the amplitudes of the constant component upon which the SMI is superposed can be brought to the same value, let's say 1, by a (noiseless) amplification. Then, the SMI signal amplitudes are given just by the modulation indexes of Eqs.3 and 4.
Interesting feature of these dependences is that the difference signal is twice the semi-sum of (absolute) amplitudes as soon as one of the two changes its sign, the case of m_1 at increasing bias. To see this, let's write Eqs.3 and 4 in the form: $m'_1= g-r$, and $m'_2=g$. Then, the difference signal is $m'_1-m'_2= -r$ at all times. But, when m'_1 changes sign, its (positive) amplitude is r-g and the semi-sum is ½ $(m'_1+m'_2)= r/2$; accordingly the ratio $|(m'_1-m'_2)| / ½(m'_1+m'_2)$ is equal to 2 (in absolute value). For clarity, a numerical example about this statement is provided in the Appendix.
In conclusion, although the amplitudes of the SMI output signals and their ratio (Eq.5) may change with gain γ – or with bias current – their difference is always double the average (or semisum) amplitude of the output signals.

3. Noise Model and calculations

We model the SMI noise with the scheme of Fig.3 bottom, which is rigorous from the point of view of second quantization, as described in Ref.[7]. The oscillating field E_0 is assumed constant in the cavity, and the coherent state fluctuation ΔE_{coh} is attributed to it. The fluctuation ΔE_{coh} is a Gaussian noise of amplitude such that the power $P_0=aE_0^2/2Z_0$ carried by the field E_0 has the classical quantum (or shot) noise, $\sigma_p^2=2h\nu P_0 B$, where B is the bandwidth of observation [6]. Explicitly, the fluctuation ΔE_{coh} has zero average, $<\Delta E_{coh}>=0$, and a quadratic mean value given by $<\Delta E_{coh}^2>=(a/2Z_0)½h\nu B$, or also a power spectral density $d<\Delta E_{coh}^2>/df=½h\nu$, of half photon per Hertz. In the following, we omit for simplicity the factor $a/2Z_0$.

Additional to the noise carried by the oscillating field, we shall consider also noises entering in the unused port of beamsplitters and partially reflecting mirrors. Indeed, for the second quantization, every port left unused is actually a port left open to the vacuum-state fluctuation, that is a field fluctuation, let us call it ΔE_{vac} (see Fig.3), equal to the coherent state fluctuation, $\Delta E_{vac} = \Delta E_{coh}$, consistent with the fact that the coherent state fluctuation ΔE_{coh} is independent from the value of the field E_0 and is therefore found also where it is $E_0=0$, .e., at unused ports [7].

With the addition of ΔE_{vac1} and ΔE_{vac2} in Fig.3, the noise model is complete [7] and we can calculate the fluctuations of output fields E_1 and E_2 as well the variance of noises superposed to output powers P_1 and P_2.

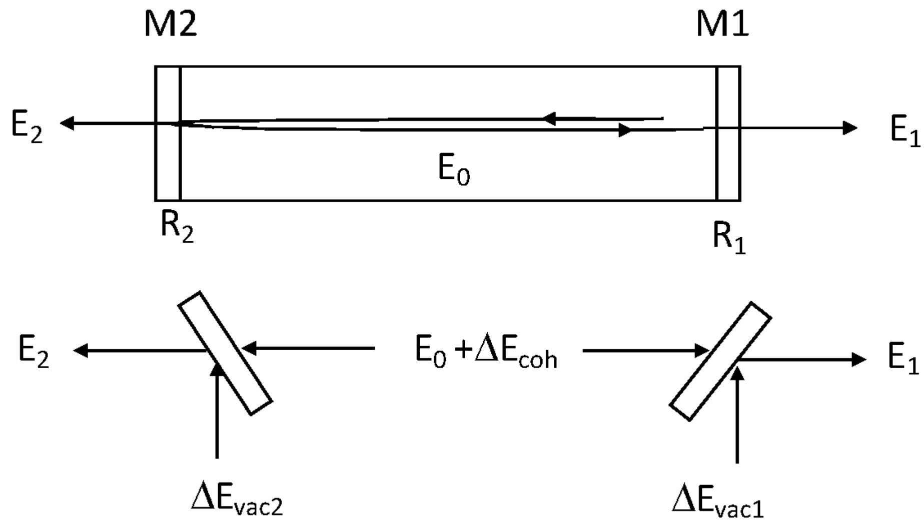

Fig. 3. Top: the laser diode cavity has mirrors with (power) reflectivity R_1 and R_2 and the optical oscillating field E_0 is assumed constant inside the cavity; bottom: the second quantization model, in which field E_0 is accompanied by the coherent state fluctuation ΔE_{coh}, and the vacuum state fluctuations $\Delta E_{vac1,2}$ enter in the unused post of the mirrors, described as beamsplitter because they have non-unitary transmission.

In the classical picture, the output powers P_1 and P_2 are affected by the shot noise due to the Poisson distribution of photons which are carried along, and the variance of the power fluctuation is given by the well-known shot-noise expression $\sigma_P^2 = 2\, h\nu\, P\, B$. As it is generated by the same power P_0 travelling back and forth in the cavity, the powers P_1 and P_2 have some correlation in their shot-noise fluctuation, but not complete correlation because the mirrors select at random which photon is transmitted and which is reflected.

In the following, we calculate the variances σ_{P1}^2 and σ_{P2}^2 for the two outputs as made up by two terms each: one totally correlated and another totally uncorrelated to the corresponding term of the other output, so that the first can be cancelled out in a differential operation and we can evaluate the SNR improvement thereafter.

With reference to Fig.3, let's now compute mean value and variance of the power delivered at output 1, $P_1=\langle| E_1^2\rangle$ (having omitted for simplicity the multiplying term $a/2Z_0$); also, for simplicity let us assume equal mirror reflectivity, $R_1=R_2=R$. Then, at mirror M_1 we can write:

$$E_1 = t\,(E_0+\Delta E_{coh}) + i\, r\, \Delta E_{vac1} \tag{6}$$

where $t=\sqrt{T}$ and $r=\sqrt{R}$ are the field transmission and reflection coefficient of the mirrors, ΔE_{coh} is the Gaussian, zero average, field fluctuation affecting E_0 (and independent from amplitude E_0) and ΔE_{vac1} is the same distribution, but uncorrelated to ΔE_{coh} , that enters as the vacuum fluctuation [7] from the unused port of the beamsplitter. Properties are:

$$\langle\Delta E_{coh})\rangle=\langle \Delta E_{vac1}\rangle =0, \text{ and } \quad \sigma_E^2=\langle\Delta E_{coh}^2\rangle=\langle\Delta E_{vac1}^2\rangle=½\, h\nu B \tag{7}$$

Now, the mean value of P_1 is given by the classical expression $P_1 \propto E^2$ but subtracted of the square average of the vacuum field (because this cannot be observed) [7]:

$$P_1 = <|E_1^2|> - <\Delta E_{vac1}^2> \quad (8)$$

Inserting (6) in (8) we get:

$$P_1 = t^2 E_0^2 + t^2<\Delta E_{coh}^2> + r^2<\Delta E_{vac1}^2> + 2t^2< E_0 E_{coh}> +2tr<E_0 E_{vac1}> +2tr<E_{coh} E_{vac1}> - <\Delta E_{vac1}^2> \quad (9)$$

and, because the 2nd, 3rd, 7th and the last term on the right-hand side cancel out, we get:

$$<P_1> = t^2 E_0^2 + 2t^2< E_0 E_{coh}> +2tr< E_0 E_{vac1}> +2tr<E_{coh} E_{vac1}>$$

As the mean value of E_{coh} and E_{vac1} are zero, E_{coh} and E_{vac1} are uncorrelated, and noting that $E_0^2 = P_0$ and $t^2 = T$ we get:

$$<P_1> = t^2 E_0^2 = T P_0 \quad (10)$$

i.e., just the expected result.

Variance is calculated as the difference $\sigma_{P1}^2 = < P_1^2 > - < P_1 >^2$, or

$$\sigma_{P1}^2 = t^4 E_0^4 + 4t^4< E_0^2 E_{coh}^2> +4t^2r^2<E_0^2 E_{vac1}^2> - t^4 E_0^4 + \text{vanishing double products}$$

Substituting $t^2=T$ and $r^2=R$, we get

$$\sigma_{P1}^2 = 4T^2E_0^2<E_{coh}^2> + 4\,TR\,E_0^2 <E_{vac1}^2> \quad (11)$$

and using $TE_0^2 = P_1$ and $<E_{coh}^2>=<E_{vac1}^2>= ½\, h\nu B$, we finally obtain

$$\sigma_{P1}^2 = 2\,T\,P_1\, h\nu\, B + 2R\,P_1\, h\nu\, B, \quad (12)$$

Worth noting, as R+T =1, (12) is also written as $\sigma_{P1}^2 = 2P_1 h\nu B$, that is, the classical variance expected for a Poisson-statistics power P_1.
But now we can repeat the calculation for exit 2, and it is straightforward to write the result as:

$$P_2 = P_1$$

$$\sigma_{P2}^2 = 4T^2E_0^2<E_{coh}^2> + 4\,TR\,E_0^2 <E_{vac2}^2>$$
$$= 2\,T\,P_2\, h\nu B + 2\,R\,P_2\, h\nu B \quad (13)$$

Note that the first right-hand side terms of (12) and (13) are the same as derive from the same process, the beating of signal with its coherent state fluctuation, so they are completely correlated and will be canceled out making the difference $P= P_1- P_2$. Instead, the second right-hand side terms of (12) and (13) are completely uncorrelated because they come from different independent fluctuations, E_{vac1} and E_{vac2}.
Taking account of the correlations, we get for the variance of $P= P_1-P_2$

$$\sigma_{P2-P1}^2 = 4T\,R\,E_0^2 <E_{vac1}^2> +4\,TR\,E_0^2 <E_{vac2}^2> = 8\,TR\,P_0\, ½\, h\nu\, B = 4R\,P_1\, h\nu\, B \quad (14)$$

to be compared to $\sigma_{P1}^2 = \sigma_{P2}^2 = 2\,P_1\, h\nu\, B$. Therefore, the ratio of free and differential variance is:

$$\sigma_{P2-P1}^2/ \sigma_{P1}^2 = 2R \quad (15)$$

and the corresponding SNR ratio, considering the doubling of differential signal becomes:

$$F = [SNR_{P2-P1}/SNR_{P1}]^2 = (4/2R)/1 = 2/R \quad (16)$$

For a semiconductor laser with a typical R=0.3 we get

$F = 2/0.3 = 6.6$ (or 8.2 dB)

About the output voltage signal $V = R_{tr}\,\sigma P$ obtained across a resistance R fed by the photodiode current $I=\sigma P$, we have for the SNR the same: tor

$[SNR_{P2-P1}/SNR_{P1}]^2=[SNR_{V2-V1}/SNR_{V1}]^2$ or also

$SNR_{V2-V1}/SNR_{V1} = \sqrt{F}$, and $20 \log\sqrt{F} = 10 \log F = 8.2$ dB

For as He-Ne laser, the front and rear outputs are in phase, in the normal operation of the source [5], so the factor 2 of the differential outputs is not achieved, and we have F=1/R. Moreover, as the reflection coefficient of typical He-Ne mirrors is R=0.95-0.98, the improvement in F is marginal.
With a slightly different method based on second quantization, Elsasser and coworkers [8] have calculated the correlations of the output fields in a Fabry-Perot laser, including the effects of internal absorption and spatial hole burning, with the aim of generating correlated light beams, and found correlation factors up to 0.8. The low-frequency suppression of 1/f components in a laser diode by output subtraction has been investigated by R.J. Fronen [9] finding almost complete correlation between the two outputs.

3.1 Extension of the noise results

Usually, Fabry-Perot semiconductor lasers have cleaved facets, so $R_1=R_2$ and the results of previous Sections apply. However, one can come across lasers with $R_1\neq R_2$ and therefore we extend here the theory to the general case of different mirror reflectivity.
On repeating the calculations of previous Section, we find that, upon equalizing the output power amplitudes, the variancesof the output difference is given by:

$$\sigma_{P2-P1}^2 = 2\,[R_2T_1+R_1T_2]\,\sqrt{(R_1R_2)}\,P_{00}\,h\nu\,B$$

where P_{00} is the power at the crossover point internal to the laser, at which left-going and right-going beams are of equal power. Moreover, the variances of the outputs – after balancing of the mean power signal – is:

$$\sigma_{P1or2}^2 = 2\,\sqrt{(T_1T_2)}\,\sqrt{(R_1R_2)}\,P_{00}\,h\nu\,B$$

hence the variance ratio becomes:

$$\sigma_{P2-P1}^2 / \sigma_{P1or2}^2 = [R_2T_1+R_1T_2] / \sqrt{T_1T_2} \qquad (15')$$

for $R_2=R_1=R$, and $T_1=T_2=T$, Eq.(16') gives the same as Eq.(15). Also, the improvement in SNR is given by $F= 2\sqrt{(T_1T_2)}/ [R_2T_1+R_1T_2]$, becomes F=1/2R for equal R and T.

3.2 Picking the front output signal

As said above, the receiving photodiode placed on the front output of mirror M1 can also serve, with its transparent window reflecting a few percent of the incoming radiation, as the target surface while intercepting practically all the power P_1 available. However, when this arrangement is not allowed by the application, normally because of its invasiveness, we can use either (i) a beamsplitter, deviating a fraction of the power in transit to the photodiode P1, as shown in Fig.4 (top), or a partial removal of the outgoing beam (see below).

The beamsplitter offers a compact solution to power pickup, because it may be as small as the beam, but has the serious disadvantage of opening a port to the vacuum fluctuation, term ΔE_{vacBS} in Fig.4 (bottom).

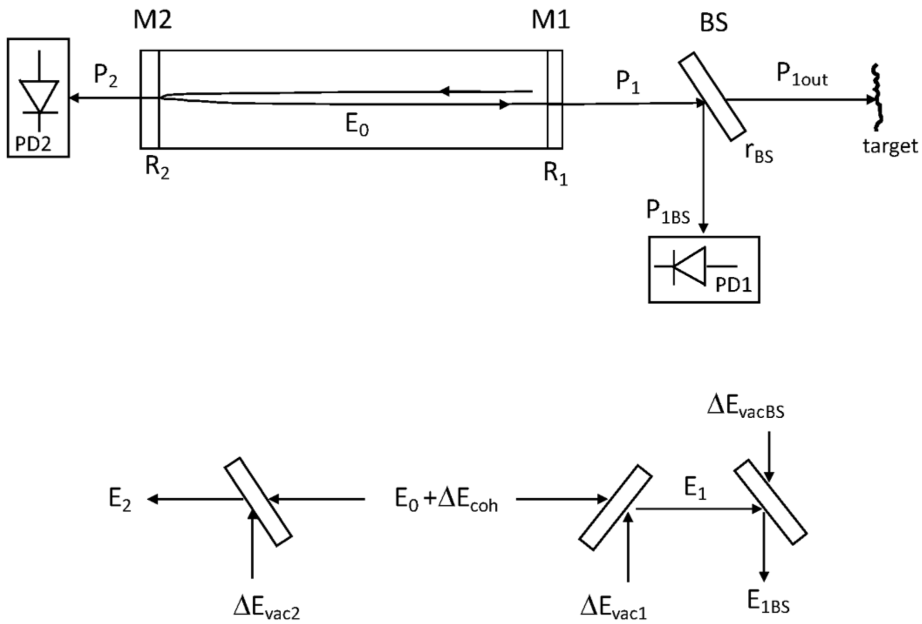

Fig. 4. (top) Pickup of the front SMI signal by means of beamsplitter BS, deviating a fraction R_{BS} of power P_1 to photodiode PD1; (bottom) equivalent circuit for the evaluation of noise, showing the added fluctuation ΔE_{vacBS} entering in the unused port of the beamsplitter.

The calculation of powers and associated variances follows the guidelines of previous Section, and for brevity we will omit here the detailed development of the analysis, limiting ourselves to report the results. For R_1=R_2=R, it is found that power at the detector PD1by is given by:

$$P_{1BS} = (r_{BS}\, t)^2 E_0^2 = R_{BS} P_1 = T R_{BS} P_0 \qquad (16)$$

while power at the other mirror is still $P_1 = t^2 E_0^2 = T P_0$, larger than P_{1BS}, and this circumstance will generally require a balance operation to get equal amplitude levels. The variance of fluctuations associated with P_{1BS} is:

$$\sigma_{P1BS}^2 = 2T R_{BS} P_{1BS} h\nu B + 2 (R R_{BS} + T_{BS}) P_{1BS} h\nu B$$
$$= 2 T R_{BS}^2 P_1 h\nu B + 2 R_{BS}(R R_{BS} + T_{BS}) P_1 h\nu B \qquad (17)$$

After the (noiseless) power amplification by a factor $1/R_{BS}$ to equalizing the amplitude of P_{1BS} before subtracting P_2. so that we obtain P_1-P_2=$2P_1$, we get for the equalized variance $\sigma_{P1BS(eq)}$:

$$\sigma_{P1BS(eq)}^2 = \sigma_{P1BS}^2 / R_{BS}^2 = \{2T R_{BS}^2 P_1 h\nu B + 2 R_{BS} (R R_{BS} + T_{BS}) P_1 h\nu B \} / R_{BS}^2$$
$$= 2T P_1 h\nu B + 2 (R + T_{BS}/R_{BS}) P_1 h\nu B \qquad (18)$$

to be compared with

$$\sigma_{P1}^2 = 2T P_1 h\nu B + 2R P_1 h\nu B$$

whence the first terms (correlated) cancels out again, and the second ones give the difference as:

$$\sigma_{P2-P1}{}^2 = 2\,(2R + T_{BS}/R_{BS})\,P_1 h\nu B$$

and $SNR_{P1-P2}{}^2 = 4/2\,(2R + T_{BS}/R_{BS})\,P_1 h\nu B$

$$= 2/(2R + T_{BS}/R_{BS})\,h\nu B \qquad (19)$$

to be compared to the single-channel $SNR_{P1}{}^2 = 1/2\,h\nu B$, whence the final result

$$F = [SNR_{P2-P1}/SNR_{P1}]^2 = 2/(R + T_{BS}/2R_{BS}) \qquad (20)$$

From Eq.20 we can see that the beamsplitter affects severely the improvement factor F. Indeed, if we chose a 50/50 beamsplitter, F would be less than 2. For the improvement to be comparable to F=2/R of the direct configuration (Fig.2), we shall limit $T_{BS}/2R_{BS}$ to a fraction of R. For example, taking T_{BS}=0.05 to have F=7.8 dB, or T_{BS}=0.10 for F=7.5 dB. At these low values of transmittance, almost all the power of the M1 output is taken by the photodiode and only a little fraction T_{BS} is used to sense the remote target. As a consequence, the SMI signal is decreased and the performance worsened, so that the improvement of F of the differential output becomes illusory.
The second method, consisting in sampling the outgoing beam by removing a small portion of it by means of a totally reflecting prism (or a mirror) is depicted in Fig.5.

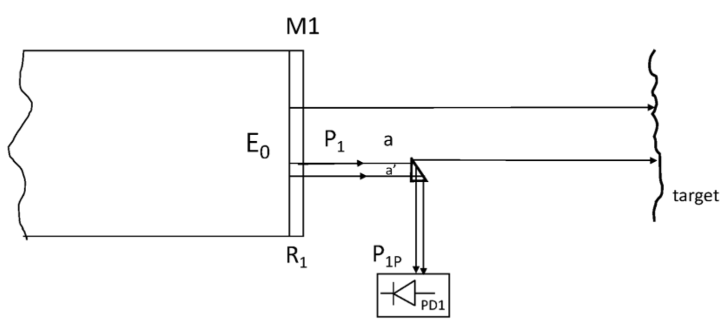

Fig.5. picking a portion a' of the beam outgoing from mirror M1 by means of a reflecting prism

The power collected by this arrangement is the ratio of areas a' and a+a' of the intercepted beam and the total beam, or P_{1P}=a'/(a+a') P_1 (fig.5). However, at equal a'/(a+a') and R_{BS}, the fractional pickup of the beam is dramatically different from the beamsplitter pickup, because it doesn't open the port to the vacuum fluctuations (as the BS in Fig.4 does). This is due to the total reflection of the prism (or of a mirror in place of it) that makes the arrangement a 2-port device instead of the 4-port of the beamsplitter (Fig.4).
Therefore, for this configuration, the expressions of variance (Eqs. 12 and 13) hold with P_1 replaced by P_{1P}, and the variance ratio of the signal difference (Eq.14) and the improvement (Eqs.15 and 16) also apply.

4. Experimental Validation

We carried out the experiment with a 650-nm diode laser, Roithner QL65D6SA with a Fabry-Perot structure. The laser had a threshold of 30 mA and was biased at 40 mA and emitted 5 mW. The monitor photodiode incorporated in the package supplied a 0.2 mA current, so it was receiving only about 10% of the power emitted by the rear mirror, and this simplified the balancing operation with the 10%=a'/(a+a') power picked up by a 1-mm side rectangular prism on the beam of about w_0=10-mm at the exit of a F=5-mm, NA=0.53 collimating lens. Photodiode PD1 was fed a transimpedance amplifier with R_{f1}=4.7-kΩ feedback resistance, and PD2 to another transimpedance amplifier feedback resistance R_{f2} adjustable between 1 and 10-kΩ. A difference op-amp provided a signal proportional to P_{P1}-P_2, and its output was directly sent to a digital oscilloscope. The target was a loudspeaker placed at 10-cm distance, with the central part covered by plain white paper. To balance the two channels, we applied a 1.5-mA triangular waveform to the bias current, and adjusted R_{f2} so as to reach the condition of equal amplitude, or near to zero difference, as shown in Fig.6.

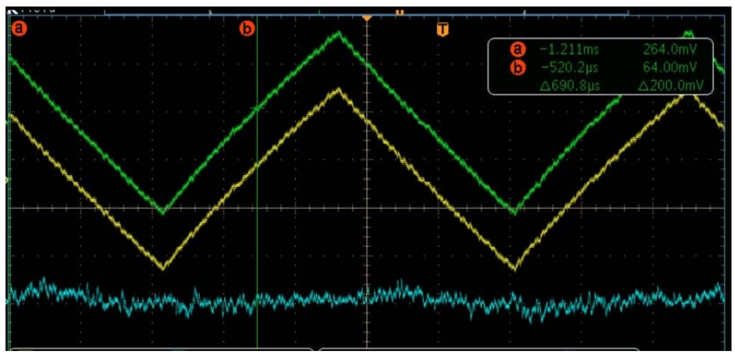

Fig.6. balancing of the two SMI signals detected by PD1and PD2: a triangular waveform is applied to the bias and generates detected responses brought to nearly identical (top trace), that is, with a residual small difference (bottom trace)

Then we analyze the difference signal P_{P1}-P_2 and its fluctuations, both in the frequency domain by means of a spectrum analyser, and as a total amplitude by means of an ac-coupled rms voltmeter.

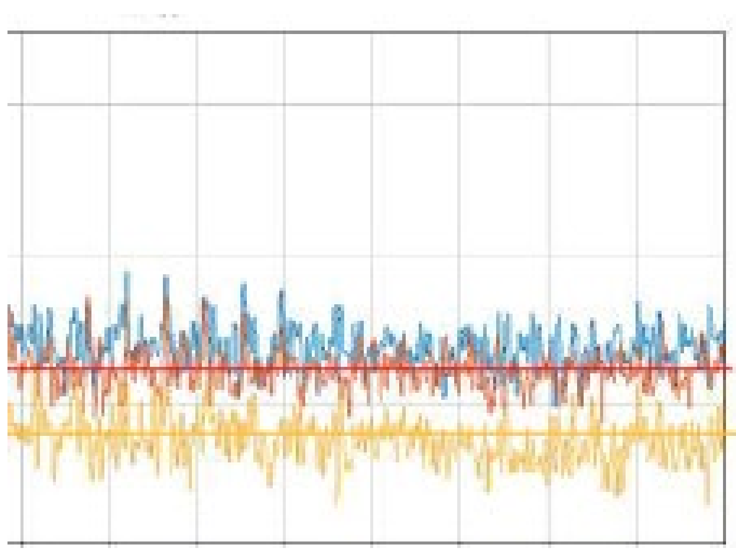

Fig.7. signal detected by PD1and PD2 and their difference, exhibiting a noise 2.5 ±1 dB smaller.

In Fig.7 we report the result of spectral noise measurement of the two channels P_{P1} and P_2, and of their difference P_{P1}-P_2, which is 2.5 dB smaller. Taking account of the doubling of signals (which amounts to 6 dB for their square, see Eq.20), the SNR improvement is 2.5+6= 8.5 ±1 dB.
We have also measured the total amplitude fluctuations of the two channels and of their difference and found that the improvement is even better than that recorded by the spectral density, typically of 2...3 dB. This is due to the presence, on both channels, of electrical (EMI) disturbances and the 1/f noise component collected almost equally by both channels and obviously cancelled by the difference operation. For example, in Fig.8 we report an example of the SMI channels deliberately disturbed by an EMI perturbation generated by the brushes of an electrical motor placed in close proximity to the optical SMI. The series of peaks at frequencies from 30 to 300 kHz are reduced in amplitude by about 25 to 30 dB thanks to the difference operation.

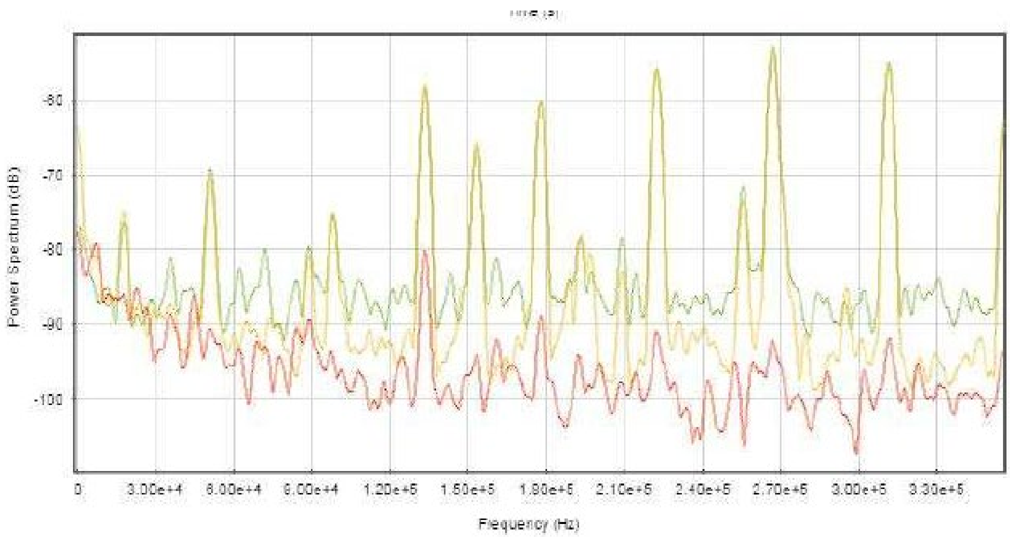

Fig.8. Peaks of EMI superposed to the SMI of channels PD1and PD2 (yellow and yellow-green) and the difference channel (red), exhibiting a disturbance reduction of 25...30 dB.

5. Conclusions

We have demonstrated that the difference signal of the two outputs – front and rear – of a laser diode SMI has an improved SNR respect to each of the two outputs. On a Fabry-Perot laser, we have measured an improvement of 8.5±1 dB, in good agreement with the theoretical value of 8.2 dB. We have found that also EMI collected by the two channels is strongly reduced (of 25...30 dB) by the difference operation. The improvement is due to the two signals being in phase opposition above threshold, and to the partial correlation of the noises as shown by an analysis based on a second-quantization model.

6. Appendix

Let's make some exemplary cases calculating the values of $m_{1,2}$ normalized to (t_1^2/r_1) $(A \cos \phi)$ using Eq.3 and 4. Let's assume for our semicondictor laser diode, $R_{1,2}$=0.3, so that ln R_1R_2=-2.40, and R_1/T_1=0.428. At threshold, $2\gamma L$ = -ln R_1R_2= 2.40. Then we have, at various values of round trip gain $2\gamma L$:

$2\gamma L$	2.40x1.1 (10% above thr)	3.60 50% above	4.80 x2	5.40 x2.25	6.00 x2.5	7.20 x3	9.60 x4
m_2 (rear)	4.17	0.83	0.42	0.33	0.28	0.21	0.114
m_1 (front)	3.74	0.4	-0.01.	-0.10	-0.15	-0.22.	-0.316
signal difference	0.43	0.43	0.43	0.43	0.43	0.43	0.43
ratio of diff to semisum	0.11	0.70	2.0	2.0	2.0	2.0	2.0

As we can see, when signal m_1 changes sign, the ratio of difference to semi-sum of amplitudes (the absolute values of m's) becomes equal to 2.

7. Conflict of Interest

The Authors declare they have no conflict of interest.

8. References

1. S. Donati: ”Developing Self-Mixing Interferometry for Instrumentation and Measurements” *Laser Photonics Rev*. **6**, pp. 393–417, DOI 10.1002/ lpor.201100002 (2012).

2. S. Donati: "Electro-Optical Instrumentation - Sensing and Measuring with Lasers", Prentice Hall, USA, ISBN 013 0161610-9, (2004).

3. S. Donati, M.Norgia: "Overview of self-mixing interferometer applications to mechanical engineering", *Optical Engineering*, **57**, 051506 (2018), DOI:10.1117/1.OE.57.5.051506

4. P.Dean, Y.L.Lim, A.Valavanis, R.Kleise, M.Nikolic, D.Indjin, Z.Ikonic, P.Harrison, A.D.Rakic, E.H.Lindfield, G.Davies: “Terahertz Imaging through Self-Mixing in a Quantum Cascade Laser”, *Optics Letters* **36**, pp.2587-2589 (2011).

5. E. Randone, S.Donati: “Self-mixing Interferometer: Analysis of the Output Signals”, *Optics Express*, **14**, pp. 9788-9796 (2006).

6.K. Li, F. Cavedo, A. Pesatori, C. Zhao, M. Norgia: "Balanced Detection for Self-Mixing Interferometry", *Optics Letters*, **42**, pp.283-285 (2017).

7. S. Donati: "Photodetectors - Devices, Circuits and Applications" 2nd ed., J.Wiley and IEEE Press, Oxford 2021, ISBN 9781119769910, see p.427-432 (2021).

8. J.L. Vey, K. Auen. W. Elsasser: "Intensity Fluctuation Correlations for a Fabry-Perot Semiconductor Laser: A Semiclassical Analysis", Opt. Comm. **146**, pp.325-338 (1998).

9. R.J. Fronen: "Correlation Between 1/f Fluctuations in the Two Output Beams of a Laser Diode", J. Quant. Electr. **27**, pp.931-936 (1991).